





## Preliminary study on the cutting force and shape error in turning of X5CrNi18-10 shafts with small feed

István Sztankovics,\*  0000-0002-1147-7475, El Majdoub Wafae  0000-0002-1147-7475

University of Miskolc, Institute of Manufacturing Science, H-3515 Miskolc, Egyetemváros

### ABSTRACT

Measuring cutting forces and shape errors is crucial for understanding and optimizing machining processes. These factors significantly describe the quality, accuracy, and efficiency of manufacturing operations. In this study, the focus is on the turning of X5CrNi18-10, a widely used austenitic stainless steel known for its excellent corrosion resistance and mechanical properties, but challenging machinability due to work-hardening tendencies and high toughness. The study investigates the effects of three key machining parameters—feed rate, depth of cut, and cutting speed—on cutting forces and shape errors, particularly cylindricity. Cutting forces directly impact tool wear, energy consumption, and surface finish, while shape errors reflect the geometric deviations from the intended design, affecting the functionality of machined components. By analyzing these parameters, the study aims to provide insights into the interactions between cutting dynamics and material behavior during turning. It evaluates how variations in feed, depth of cut, and cutting speed influence the magnitude of cutting forces and the resulting geometric precision. These findings contribute to the development of optimized machining strategies, ensuring improved dimensional accuracy, reduced tool wear, and enhanced overall process stability for X5CrNi18-10 and similar materials.

### ARTICLE INFO

Received: 1 October 2024  
Revised: 30 November 2024  
Accepted: 10 December 2024

### KEYWORDS:

Cutting force;  
Cylindricity;  
Design of experiments;  
Longitudinal turning;  
Shape accuracy.

\*Corresponding author's e-mail:  
[istvan.sztankovics@uni-miskolc.hu](mailto:istvan.sztankovics@uni-miskolc.hu)

### 1. INTRODUCTION

Turning is a fundamental machining process [1] widely used in the manufacturing industry for producing cylindrical components with precise dimensions and surface quality. Among the critical aspects that influence the efficiency and outcome of turning operations are cutting forces and shape errors [2]. Understanding these parameters and their relationship is necessary for optimizing machining processes, ensuring product quality, and enhancing tool life. This study focuses on the cutting forces and shape errors that arise during the turning of X5CrNi18-10 stainless steel shafts at small feed rates, an area of significant practical and scientific interest.

Cutting forces in turning are the forces generated by the interaction between the cutting tool and the workpiece material. These forces are typically decomposed into three components: radial (perpendicular to the workpiece surface), tangential (parallel to the cutting direction and responsible for energy consumption), and axial (along the

axis of the workpiece) [3,4]. The magnitude and direction of these forces depend on several factors, including cutting speed, feed rate, depth of cut, tool geometry, and the properties of the workpiece material. Cutting forces play a central role in determining tool wear, surface finish, and dimensional accuracy [2,5]. Excessive cutting forces can lead to premature tool failure, increased power consumption, and poor surface quality. In contrast, an understanding of these forces allows for the optimization of cutting parameters, ensuring efficient material removal while maintaining the desired quality [7,8]. Particularly in operations with small feed rates, cutting forces tend to be less intense, but their influence on precision and shape errors becomes more pronounced.

Shape errors, or geometric deviations, refer to inconsistencies between the intended and actual dimensions or profiles of the machined surface. In turning, common shape errors include cylindricity errors, roundness deviations, and taper [9]. These errors can arise from various sources, such as tool deflection, machine

vibrations, thermal deformation, and inaccuracies in the cutting parameters [10,11]. Cylindricity error is of particular importance in applications requiring high precision, as it directly impacts the functionality and assembly of the machined component [12,13]. Factors such as cutting force variations, uneven material removal, and tool wear contribute significantly to these deviations. Moreover, when machining at small feed rates, the precision of the operation is heavily influenced by the relationship between cutting dynamics and material properties [14], making it crucial to study shape errors in this context.

The relationship between cutting forces and shape errors is a critical area of study in precision machining [15,16]. Cutting forces not only influence the material removal process but also determine the extent of tool deflection and vibration, both of which are primary contributors to shape errors. For instance, an increase in cutting forces can lead to greater tool deflection, resulting in geometric inaccuracies on the machined surface [17,18]. Similarly, variations in cutting forces can induce uneven material removal, further exacerbating shape errors. By studying the connection between cutting forces and shape errors, it becomes possible to predict and control geometric deviations, optimize machining parameters, and improve overall process stability [19,20]. Such insights are particularly valuable in high-precision industries, such as aerospace, automotive, and medical device manufacturing, where even minor deviations can compromise the functionality and performance of critical components.

X5CrNi18-10, commonly known as AISI 304 stainless steel, is an austenitic stainless steel widely used for its excellent corrosion resistance, high toughness, and good mechanical properties [21]. It is a preferred material in various industries, including food processing, chemical, and medical, due to its durability and ability to withstand harsh environments. However, the machinability of X5CrNi18-10 poses significant challenges. One of the primary difficulties in machining X5CrNi18-10 is its tendency to work-harden rapidly during cutting [22]. This phenomenon increases the cutting forces required and accelerates tool wear [23,24], making it challenging to maintain dimensional accuracy and surface finish. Additionally, the high ductility and toughness of the material can lead to issues such as built-up edge formation and poor chip evacuation, further complicating the machining process. When turning X5CrNi18-10 shafts at small feed rates, these challenges are amplified due to the reduced material removal rate and increased sensitivity to tool vibrations and deflection. As a result, understanding the cutting forces and their influence on shape errors becomes even more critical for achieving precision and efficiency in machining this material.

This study addresses a critical gap in understanding the interaction between cutting forces and shape errors in turning operations involving X5CrNi18-10 shafts at small feed rates. While extensive research has been conducted on cutting forces and shape errors independently, limited studies have explored their relationship, especially in the context of difficult-to-machine materials like X5CrNi18-

10. By investigating this relationship, the study aims to provide a comprehensive basis for optimizing machining parameters to minimize shape errors and cutting forces simultaneously. The findings will not only contribute to improving the machinability of X5CrNi18-10 but also enhance the overall efficiency and precision of turning operations. The primary objectives of this study are as follows:

1. To measure and analyse the major cutting force generated during the turning of X5CrNi18-10 shafts at small feed rates.
2. To evaluate the shape errors, with a particular focus on cylindricity, resulting from variations in cutting parameters.

By addressing these objectives, the study seeks to advance the understanding of precision machining dynamics and contribute to the development of optimized machining strategies for X5CrNi18-10 and similar materials.

In summary, this research highlights the critical role of cutting forces and their impact on shape errors in turning operations. It focuses on the challenges and opportunities associated with machining X5CrNi18-10 at small feed rates, providing valuable insights for improving precision and efficiency in industrial applications.

## 2. EXPERIMENTAL CONDITIONS AND METHODS

The aim of the study was to investigate the effects of cutting parameters on the cutting force and shape error in the turning process. In this research, both the cutting experiment and theoretical evaluation were utilized to achieve the result and accomplish the study. During the experiment, three parameters were varied to be analyzed in the study: cutting speed ( $v_c$ ) varied in two levels (200, 300 m/min), the feed ( $f$ ) varied in two levels (0.08, 0.3 mm/rev.), and the depth of cut ( $a$ ) varied in two levels (0.5 and 1 mm). The selected parameters are shown in Table 1.

**Table 1** – Experimental setups and the transformed values.

Setup	1	2	3	4	5	6	7	8
Selected values of the setup parameters								
$f \left[ \frac{mm}{rev} \right]$	0.08	0.3	0.08	0.3	0.08	0.3	0.08	0.3
$v_c \left[ \frac{m}{min} \right]$	200	200	300	300	200	200	300	300
$a \left[ mm \right]$	0.5	0.5	0.5	0.5	1	1	1	1
Transformed values of the setup parameters								
$f' [-]$	-1	1	-1	1	-1	1	-1	1
$v_c' [-]$	-1	-1	1	1	-1	-1	1	1
$a' [-]$	-1	-1	-1	-1	1	1	1	1

Stainless steel X5CrNi18.10 with a hardness value of 310HV10 was the selected material of the machining workpiece. The designation stands for the chromium-nickel austenitic stainless steel known for its excellent corrosion resistance provided by the chromium element. The workpieces with an outer diameter of 50 mm were separated into equal sections of 30 mm by 5 mm grooves that were machined to measure the cutting force in three directions. The following-mentioned equipment was set up together to obtain cutting force data. HAAS model ST-

20Y-EU lathe was used to perform the experiment in a lubricated condition with utilization a 5% emulsion of "CIKS HKF 420" type coolant oil. DNMG150604-MF1 CP500 carbide/ceramic with a negative shape insert was mounted to the DDJNL2525M15 tool holder and used to accomplish the stable condition for machining. This type of tool is suitable for heavy and rough cut of various materials.

The measured data was obtained by mounting a dynamometer on the turret head of the machine and fixing the cutting tool on it using a suitable tool holder. The cutting force generated was broken into three forces ( $F_c$  cutting force,  $F_p$  passive force, and  $F_f$  feed force) and captured by connecting three charge amplifiers to a dynamometer in the aim of converting the electric signals to a proportional output voltage ready for analysis. To get all the data, shape error measurements were needed, and a Talyrond 365 precision measuring instrument was used with parameters based on standard protocols and previous studies measurements. Measurements were taken across nine planes with a 2.75 mm separation between each, resulting in the measurement of a cylinder with a 22.0 mm axial length per run.

The following parameters were analyzed (where the shape errors are defined in the ISO 12180-1 standard):

- $F_c$  – major cutting force, part of the cutting force and tangential to the machined surface [N]
- $\sigma_{F_c}$  – standard deviation of the major cutting force, which is calculated during the constant phase [N]
- $CYLt$  – Cylindricity, the minimum radial separation of two cylinders, coaxial with the fitted reference axis [ $\mu\text{m}$ ]
- $CYLtt$  – Cylinder Taper, the absolute difference in diameters measured between two specially constructed straight lines at the top and bottom of the cylinder [ $\mu\text{m}$ ]

Polynomial equations were derived to calculate and represent the analyzed parameters, as shown in Equation 1. This equation incorporates the variables ( $f$ ,  $v_c$ ,  $a$ ), along with their interactions, while the constants ( $k_i$ ) quantify the contribution of each factor.

$$y(f, v_c, a) = k_0 + k_1f + k_2v_c + k_3a + k_{12}fv_c + k_{13}fa + k_{23}v_c a + k_{123}fv_c a \quad (1)$$

The parameters are represented by the function  $y(f, v_c, a)$  in this context. These equations quantify and illustrate the impact of cutting speed, feed rate, and depth of cut on the geometric characteristics of machined surfaces. They offer a systematic basis for analyzing and optimizing machining processes to achieve targeted dimensional accuracy and surface quality.

**Table 2** – Force and shape error measurement results.

Setup	1	2	3	4	5	6	7	8
$F_c$ [N]	130.2	425.3	121.6	364.7	131.6	735.0	229.4	671.9
$\sigma_{F_c}$ [N]	1.50	3.82	1.84	2.77	2.07	6.96	2.26	9.70
$CYLt$ [ $\mu\text{m}$ ]	8.6	17.5	3.7	12.4	9.4	13.7	4.5	21.3
$CYLtt$ [ $\mu\text{m}$ ]	12.8	18.8	4.9	-3.52	14.9	-4.1	7.8	-26.4

### 3. RESULTS

During the completion of the designated research work the following evaluations were carried out. The generated cutting force data was plotted using python code. The mean ( $F_c$ ) and the standard deviation ( $\sigma_{F_c}$ ) of the major cutting force were calculated. This indicates the variation of the data in relation to the mean. As well as following the mentioned methodology in the previous sections the shape error parameters selected to be analyzed are Total Cylindricity Error ( $CYLt$ ) and Cylindrical Taper ( $CYLtt$ ). All previously described calculated and measured values of the parameters are presented in Table 2.

The calculation formulas based on Equation 1 were also determined for the studied output parameters, which aids the discussion section. The major cutting force in the studied range is determined by Equation 2.

$$F_c(f, v_c, a) = 404.9 - 577.0f - 1.356v_c - 805.2a + 2.585fv_c + 4781.1fa + 2.920v_c a - 9.897fv_c a \quad (2)$$

The mathematical representation of the standard deviation of the major cutting force is shown in Equation 3.

$$\sigma_{F_c}(f, v_c, a) = -3.839 + 47.34f + 0.0242v_c + 5.59a - 0.2422fv_c - 48.27fa - 0.03166v_c a + 0.3581fv_c a \quad (3)$$

The total cylindricity error is determined by Equation 4.

$$CYLt(f, v_c, a) = 3.783 + 177.6f - 0.00393v_c + 22.93a - 0.5819fv_c - 272.0fa - 0.0904v_c a + 1.152fv_c a \quad (4)$$

The cylinder taper is calculated by the application of Equation 5.

$$CYLtt(f, v_c, a) = 7.10 + 263.7f - 0.0381v_c + 17.93a - 0.6157fv_c - 211.5fa - 0.02191v_c a - 0.0763618fv_c a \quad (5)$$

### 4. DISCUSSION

The next step involves analyzing the collected data after outlining the research methods, equipment, measured results, and equations. This analysis is carried out in two stages:

- **Main Effects Analysis:** This initial stage examines how the cutting parameters—feed, cutting speed, and depth of cut—impact the cutting force and shape error parameters, such as cylindricity.
- **Surface Diagram Analysis:** In the second stage, surface diagrams are plotted based on the equations presented earlier in the paper. These diagrams are evaluated to illustrate the influence of variations in cutting parameters on the measured cutting speed and cylindricity parameters during the experiment.

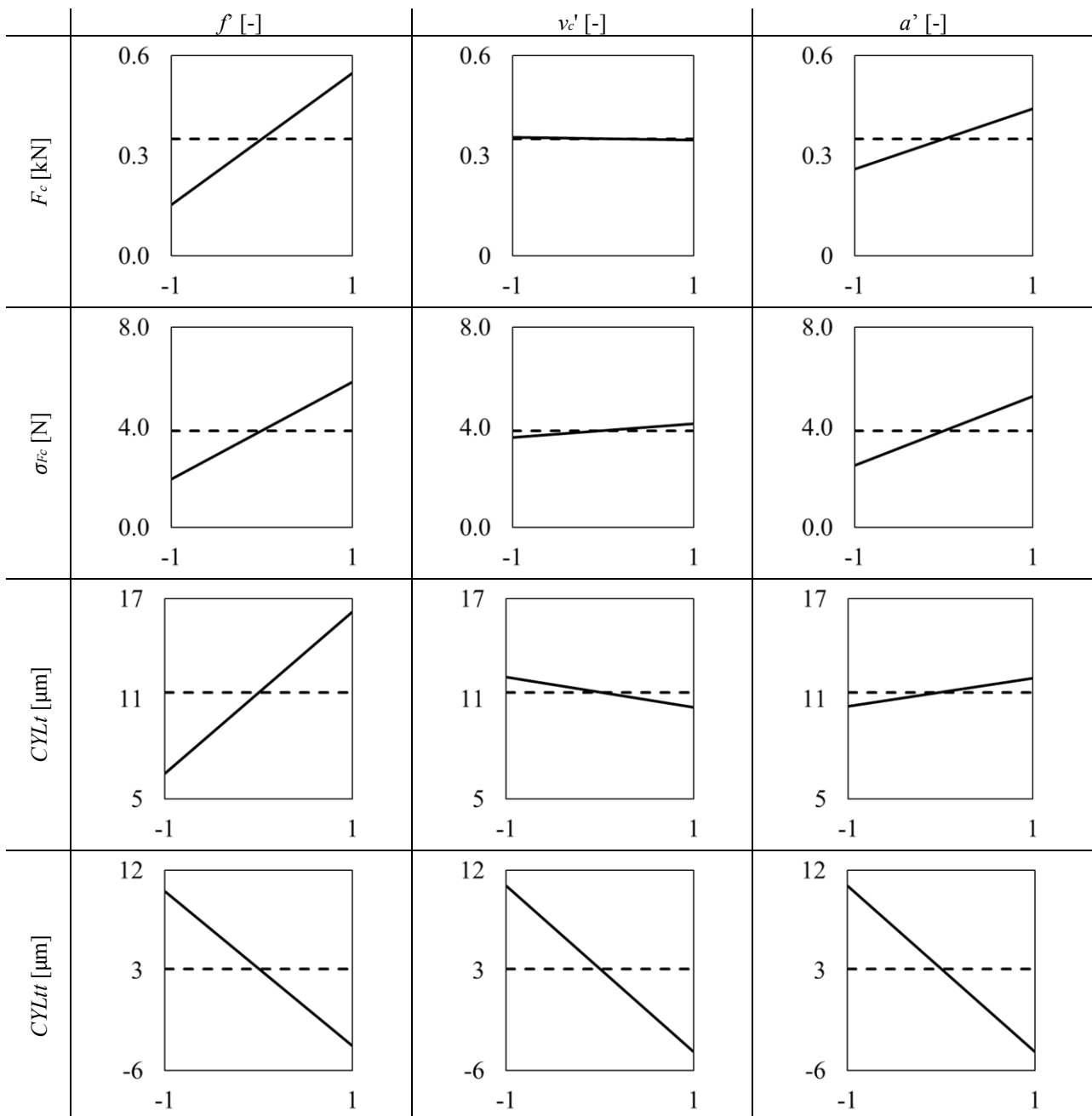


Fig. 1 The total cylindricity error in function of the studied variables

#### 4.1 Main effect analysis

In the goal of evaluating the influence of the cutting parameters on the cutting force and cylindricity, the main effect plots were generated and each parameter was analyzed separately using the plots presented in Figure 1. The methodology utilized to obtain the graphs includes several steps starting by calculating the mean of averaged values and presented as dashed line. Then two means from three cutting parameters were generated: one in the lower limit (-1) and the other one in upper limit (1) which connected by solid or continuous line. The direction and

slope show how the cutting parameters influence the cutting force and the cylindricity in the aim of optimizing the cutting setting for better precision.

First, the main effect of the feed change is analyzed. Figure 1 shows that increasing the feed can increase the cutting force, standard deviation, and total cylindricity  $CYL_t$  due to the higher material resistance and tool vibrations. However, when the feed rises, the cylindricity taper decreases. That can be explained by increasing the feed, which can amplify imperfections and reduce precision.

Examining the second column of the graphs in Figure 1 gives the effects of cutting speed on other parameters. Raising the cutting speed can slightly increase the total

cylindricity but decrease the cylindricity taper. However, it seems that increasing the cutting speed has a minor impact on the standard deviation and no relation with cutting force, which is directly affected by feed and depth of cut. Finally, the influence of the depth of cut is studied, and the graphs in the last column of Figure 1 represent the results. The depth of cut influences the parameters in the same way as the feed with different slopes. The force parameters increase with increasing depth of cut. While the cylindricity error slightly increases with rising the depth of cut. But the cylindricity taper decreases.

**4.2 Detailed analysis of the technological parameters**

Following the evaluation of the main effects, the detailed analysis of cutting speed, feed and depth of cut is conducted. As well as the surface plots are generated to observe how the variation of the cutting parameters affects the cutting force and the shape error parameters. A comparative evaluation was created by plotting separate graphs by depth of cut in two levels 0.5 mm and 1 mm.

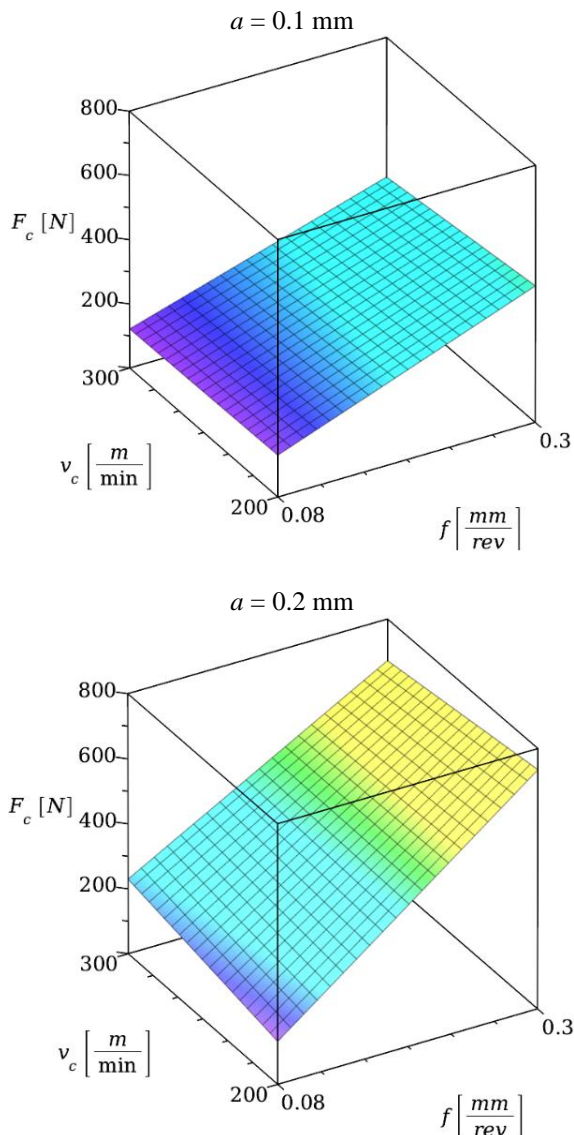


Fig. 2 The major cutting force in function of the studied variables

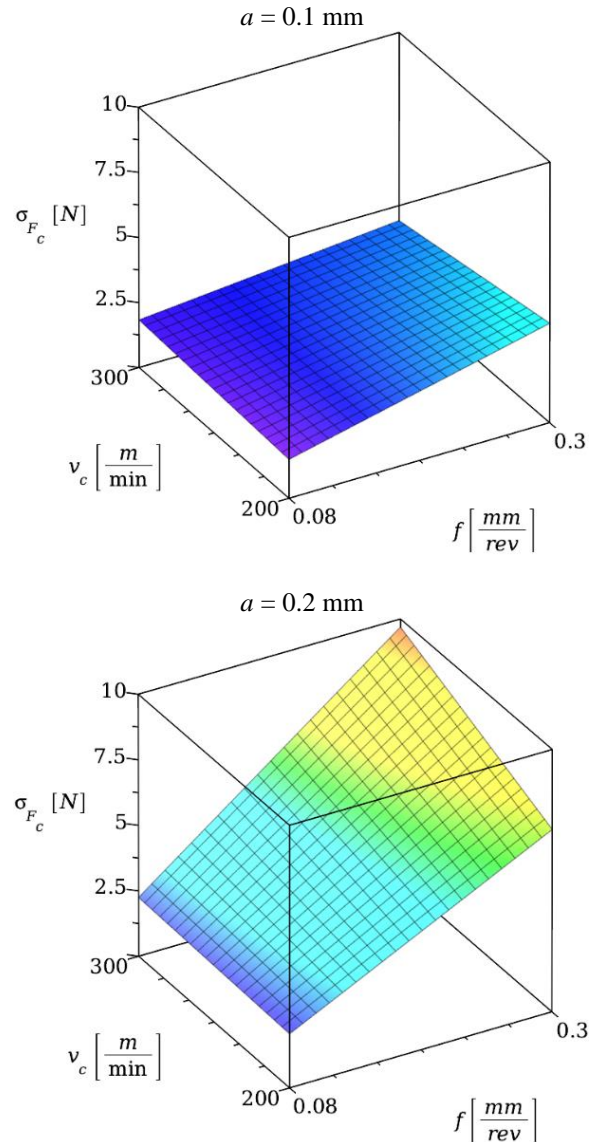


Fig. 3 The standard deviation of the major cutting force in function of the studied variables

Figure 2 represents the changes of  $F_c$  as a function of the studied variables. It is obvious that doubling the depth of cut significantly increases the cutting force, almost two-fold, as well as when the feed rises from 0.08 to 0.3 mm/rev., cutting force is increased by three folds. However, at lower depth of cut of 0.5 mm, there is almost no effect on the cutting force when the speed went from 200 m/min to 300 m/min, but by increasing the feed to 1 mm there a slight change with the change in speed.

The variation of the standard deviation as a function of feed, cutting speed, and depth of cut is shown in Figure 3. Particularly, three-fold of standard deviation has increased by raising the depth of cut from 0.5 mm to 1 mm at a cutting speed of 300 m/min. In lower depth of cut, the standard deviation has slightly increased by raising the feed, but even with an increase in the cutting speed, the standard deviation remains constant. While at the higher depth of cut, changing the feed from 0.08 mm/rev. to 0.3 mm/rev. amplifies the standard deviation three-fold.

Figure 4 represents the influence of cutting speed, feed, and depth of cut on the total cylindricity. Raising the depth of cut shows an increase of 3.5-fold in the *CYLt* at a cutting speed of 300 m/min and at the feed of 0.3 mm/rev. In lower feed of 0.08 mm/rev., increasing speed has a minor lowering effect on the *CYLt*, as well as the feed tends to have an increasing effect on *CYLt* at a lower speed of 200 m/min.

Figure 5 represents the analysis of total cylindricity taper as a function of feed, cutting speed, and depth of cut. The results highlight that total cylindricity taper decreases as the three parameters studied increase. At the upper limit of the depth of cut (1 mm), a twofold reduction in *CYLt* is visualized when the cutting speed is 300 m/min. In addition, both cutting speed and feed illustrate a noticeable effect in reducing *CYLt*. Furthermore, at the lower limit of the depth of cut (0.5 mm), the *CYLt* shows stable behavior at a smaller feed rate of 0.8 mm/rev., even with an increase in speed. However, at a higher feed rate of 0.3 mm/rev., *CYLt* decreases by approximately 50%.

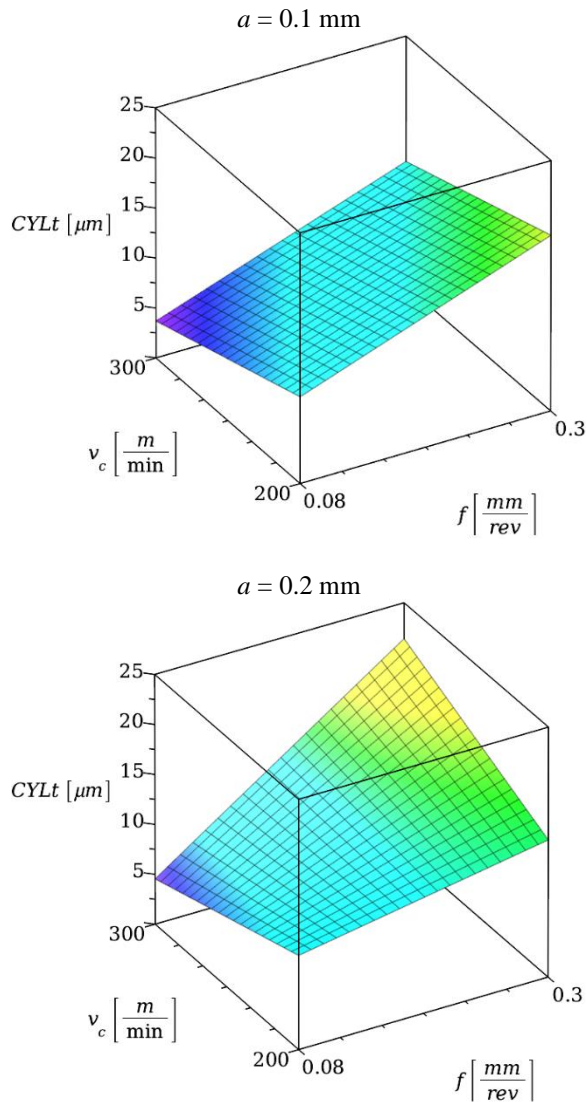


Fig. 4 The *CYLt* error in function of the studied variables

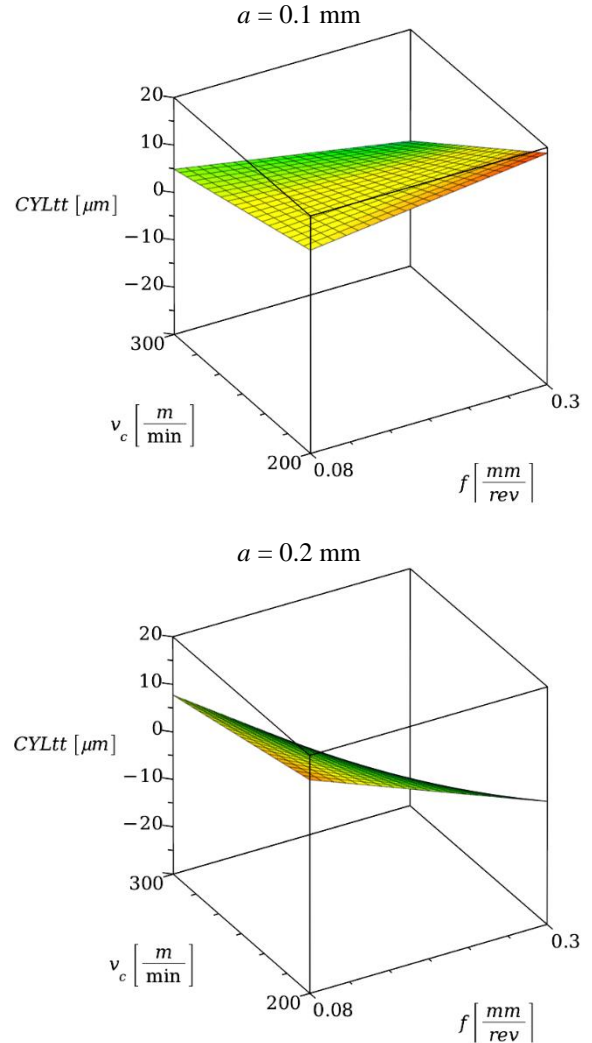


Fig. 5 The *CYLt* error in function of the studied variables

## 5. CONCLUSIONS

This study focused on the effects of machining parameters—feed rate, cutting speed, and depth of cut—on cutting forces and shape errors during the turning of X5CrNi18-10 stainless steel. Using experimental and theoretical approaches, key insights into the relationships between machining conditions and output parameters were established. The findings revealed that increasing the feed rate and depth of cut significantly influences cutting forces, particularly the major cutting force ( $F_c$ ), and its variation. The cutting speed had a less pronounced effect on cutting forces but showed subtle impacts on shape errors. Cylindricity (*CYLt*) and cylindricity taper (*CYLt*) were used to evaluate shape errors, with results indicating that higher feed rates and depth of cut increased cylindricity errors while reducing cylindricity taper.

The derived polynomial equations allowed for a systematic quantification of these interactions, providing a valuable tool for predicting cutting forces and shape errors under varying machining conditions. The analysis highlighted that feed rate and depth of cut are the dominant factors

affecting cutting forces, whereas all three parameters collectively influence shape errors.

Overall, the study contributes to the optimization of machining processes for X5CrNi18-10, offering practical guidelines for achieving improved dimensional accuracy in turning operations.

## ACKNOWLEDGEMENTS

This research was supported by project No. 2020-1.2.3-EUREKA-2022-00025 which was realized with financial help of the National Research Development and Innovation Fund of the Ministry of Culture and Innovation of Hungary.

## REFERENCES

- [1] Juneja, B. L. (2003). *Fundamentals of metal cutting and machine tools*. New Age International.
- [2] Ramesh, R., Mannan, M. A., & Poo, A. N. (2000). Error compensation in machine tools—a review: part I: geometric, cutting-force induced and fixture-dependent errors. *International Journal of Machine Tools and Manufacture*, vol. 40, no. 9, p. 1235–1256. DOI: 10.1016/S0890-6955(00)00009-2.
- [3] Ee, K., Balaji, A., Li, P., & Jawahir, I. (2001). Force decomposition model for tool-wear in turning with grooved cutting tools. *Wear*, vol. 249, no. 10–11, p. 985–994. DOI: 10.1016/S0043-1648(01)00837-7.
- [4] Kunderák, J., Markopoulos, A. P., Makkai, T., & Karkalos, N. E. (2019). Effect of edge geometry on cutting forces in face milling with different feed rates. *Manufacturing Technology*, vol. 19, no. 6, p. 984–992. DOI: 10.21062/ujep/407.2019/a/1213-2489/mt/19/6/984.
- [5] Astakhov, V. P. (2004). The assessment of cutting tool wear. *International Journal of Machine Tools and Manufacture*, vol. 44, no. 6, p. 637–647. DOI: 10.1016/j.ijmachtools.2003.11.006.
- [6] Ezugwu, E. (2005). Key improvements in the machining of difficult-to-cut aerospace superalloys. *International Journal of Machine Tools and Manufacture*, vol. 45, no. 12–13, p. 1353–1367. DOI: 10.1016/j.ijmachtools.2005.02.003.
- [7] Li, X., Liu, X., Yue, C., Liang, S. Y., & Wang, L. (2022). Systematic review on tool breakage monitoring techniques in machining operations. *International Journal of Machine Tools and Manufacture*, vol. 176, p. 103882. DOI: 10.1016/j.ijmachtools.2022.103882.
- [8] Karpuschewski, B., Kunderák, J., Varga, G., Deszpoth, I., & Borysenko, D. (2018). Determination of specific cutting force components and exponents when applying high feed rates. *Procedia CIRP*, vol. 77, p. 30–33. DOI: 10.1016/j.procir.2018.08.199.
- [9] Smith, G. T. (2002). Roundness and cylindricity. In *Industrial Metrology*, p. 135–184. DOI: 10.1007/978-1-4471-3814-3\_4.
- [10] Liu, Q., Zhang, C., & Wang, H. B. (1997). Form-accuracy analysis and prediction in computer-integrated manufacturing. *International Journal of Machine Tools and Manufacture*, vol. 37, no. 3, p. 237–248. DOI: 10.1016/S0890-6955(96)00068-5.
- [11] Singaravel, B., Marulaswami, C., & Selvaraj, T. (2016). Analysis of the effect of process parameters for circularity and cylindricity errors in turning process. *Applied Mechanics and Materials*, vol. 852, p. 255–259. DOI: 10.4028/www.scientific.net/amm.852.255.
- [12] Weihua, N., & Zhenqiang, Y. (2012). Cylindricity modeling and tolerance analysis for cylindrical components. *The International Journal of Advanced Manufacturing Technology*, vol. 64, no. 5–8, p. 867–874. DOI: 10.1007/s00170-012-4078-3.
- [13] Cho, N., & Tu, J. (2002). Quantitative circularity tolerance analysis and design for 2D precision assemblies. *International Journal of Machine Tools and Manufacture*, vol. 42, no. 13, p. 1391–1401. DOI: 10.1016/S0890-6955(02)00080-9.
- [14] Sun, X., Yao, P., Qu, S., Yu, S., Zhang, X., Wang, W., Huang, C., & Chu, D. (2022). Material properties and machining characteristics under high strain rate in ultra-precision and ultra-high-speed machining process: a review. *The International Journal of Advanced Manufacturing Technology*, vol. 120, no. 11–12, p. 7011–7042. DOI: 10.1007/s00170-022-09111-5.
- [15] Agarwal, A., & Desai, K. (2020). Predictive framework for cutting force induced cylindricity error estimation in end milling of thin-walled components. *Precision Engineering*, vol. 66, p. 209–219. DOI: 10.1016/j.precisioneng.2020.07.007.
- [16] Abas, M., Salah, B., Khalid, Q. S., Hussain, I., Babar, A. R., Nawaz, R., Khan, R., & Saleem, W. (2020a). Experimental investigation and statistical evaluation of optimized cutting process parameters and cutting conditions to minimize cutting forces and shape deviations in AL6026-T9. *Materials*, vol. 13, no. 19, p. 4327. DOI: 10.3390/ma13194327.
- [17] Ryu, S. H., Lee, H. S., & Chu, C. N. (2003). The form error prediction in side wall machining considering tool deflection. *International Journal of Machine Tools and Manufacture*, vol. 43, no. 14, p. 1405–1411. DOI: 10.1016/S0890-6955(03)00183-4.
- [18] Benardos, P., Mosialos, S., & Vosniakos, G. (2006). Prediction of workpiece elastic deflections under cutting forces in turning. *Robotics and Computer-Integrated Manufacturing*, vol. 22, no. 5–6, p. 505–514. DOI: 10.1016/j.rcim.2005.12.009.
- [19] Zhao, Z., Wang, S., Wang, Z., Wang, S., Ma, C., & Yang, B. (2020). Surface roughness stabilization method based on digital twin-driven machining parameters self-adaption adjustment: a case study in five-axis machining. *Journal of Intelligent Manufacturing*, vol. 33, no. 4, p. 943–952. DOI: 10.1007/s10845-020-01698-4.
- [20] Zhang, Z., Yang, Y., Li, G., Qi, Y., Yue, C., Hu, Y., & Li, Y. (2022). Machining accuracy reliability

- evaluation of CNC machine tools based on the milling stability optimization. *The International Journal of Advanced Manufacturing Technology*, vol. 124, no. 11–12, p. 4057–4074. DOI: 10.1007/s00170-022-08832-x.
- [21] Walczak, M., Szala, M., & Okuniewski, W. (2022). Assessment of corrosion resistance and hardness of shot peened X5CRNI18-10 steel. *Materials*, vol. 15, no. 24, p. 9000. DOI: 10.3390/ma15249000.
- [22] Patel, U. S., Rawal, S. K., Arif, A., & Veldhuis, S. C. (2020). Influence of secondary carbides on microstructure, wear mechanism, and tool performance for different cermet grades during high-speed dry finish turning of AISI 304 stainless steel. *Wear*, vol. 452–453, p. 203285. DOI: 10.1016/j.wear.2020.203285.
- [23] Pálmai, Z., Kunderák, J., Felhő, C., & Makkai, T. (2024). Investigation of the transient change of the cutting force during the milling of C45 and X5CrNi18-10 steel taking into account the dynamics of the electro-mechanical measuring system. *The International Journal of Advanced Manufacturing Technology*, vol. 133, no. 1–2, p. 163–182. DOI: 10.1007/s00170-024-13640-6.
- [24] França, P. H., Barbosa, L. M., Fernandes, G. H., Machado, Á. R., Martins, P. S., & Da Silva, M. B. (2024). Internally cooled tools: an eco-friendly approach to wear reduction in AISI 304 stainless steel machining. *Wear*, vol. 554–555, p. 205490. DOI: 10.1016/j.wear.2024.205490.
- [25] Taylor Hobson (2011). Exploring Roundness - A fundamental guide to the measurement of cylindrical form. *Taylor Hobson Limited*, Leicester, England, p. 100.